

Sasa Sofyan Munawar · Kenji Umemura · Shuichi Kawai

## Characterization of the morphological, physical, and mechanical properties of seven nonwood plant fiber bundles

Received: May 11, 2006 / Accepted: July 28, 2006 / Published online: December 10, 2006

**Abstract** The morphological, physical, and mechanical properties of the nonwood plant fiber bundles of ramie, pineapple, sansevieria, kenaf, abaca, sisal, and coconut fiber bundles were investigated. All fibers except those of coconut fiber had noncircular cross-sectional shapes. The cross-sectional area of the fiber bundles was evaluated by an improved method using scanning electron microscope images. The coefficient factor defined as the ratio of the cross-sectional area determined by diameter measurement, to the cross-sectional area determined by image analysis was between 0.92 and 0.96 for all fibers. This indicated that the area determined by diameter measurement was available. The densities of the fiber bundles decreased with increasing diameters. The diameters of each fiber species had small variation of around 3.4%–9.8% within a specimen. The tensile strength and Young's modulus of ramie, pineapple, and sansevieria fiber bundles showed excellent values in comparison with the other fibers. The tensile strength and Young's modulus showed a decreasing trend with increasing diameter of fiber bundles.

**Key words** Plant fiber · Physical properties · Mechanical properties · Morphological characteristic · Cross-sectional area

### Introduction

Among the natural fibers obtained from annual nonwood plant fibers, the bast fibers (flax, hemp) have extraordinary high mechanical strength.<sup>1</sup> The mechanical properties of

plant fibers depend on their physical, chemical, and morphological properties such as the fiber orientation, cellulose content, crystal structure and diameter/cross-sectional area of the fiber.<sup>2</sup> These natural fibers have potential to be applied as reinforcement materials to composite products.

The single unit fiber test and the fiber-bundle test have been established for the evaluation of fiber strength. The single unit fiber test gives exact results, but the fiber-bundle test has some advantages of being faster, easier, and practical use in application. The test results depend generally on the various parameters, such as the testing time and rate, influence of the clamp, and determination of the fiber cross-sectional area.<sup>3</sup> The fiber cross-sectional area strongly influences the fiber strength. However, the methods used for determining the fiber cross-sectional area have not been fully exploited.

In this article, the evaluation method for measuring the cross-sectional area of fiber bundles is discussed. The physical, mechanical, and morphological properties of various nonwood plant fiber bundles were characterized to find the appropriate natural fibers that can be used for reinforcement of composite products. Thus, relationships among density, diameter, and mechanical and morphological properties of fibers are discussed.

### Materials and methods

#### Materials

Seven nonwood plant fiber bundles, i.e. abaca (*Musa textiles* Nee.) leaf fiber (AL), pineapple [*Ananas comosus* (L.) Merr] leaf fiber (PL), sansevieria (*Sansevieria trifasciata* Prain) leaf fiber (SaL), sisal (*Agave sisalana* Perrina) leaf fiber (SiL) from Subang in West Java, Indonesia, coconut (*Cocos nucifera* L.) husk fiber (CH) from Tasikmalaya in West Java, Indonesia, kenaf (*Hibiscus cannabinus* L.) bast fiber (KB) from Lamongan in East Java, Indonesia, and ramie [*Boehmeria nivea* (L.) Gaudich] bast fiber (RB) from Wonosobo in Central Java, Indonesia, were used for the

S.S. Munawar (✉) · K. Umemura · S. Kawai  
Research Institute for Sustainable Humanosphere, Kyoto University,  
Gokasho, Uji, Kyoto 611-0011, Japan  
Tel. +81-774-38-3670; Fax +81-774-38-3678  
e-mail: sasasofyan@rish.kyoto-u.ac.jp

Part of this report was presented at the 6th International Wood Science Symposium, LIPI-JSPS Core University Program, Bali, Indonesia, 29–31 August 2005

experiment. The AL, PL, SaL, SiL, RB, and CH samples underwent a decortication process and the KB sample underwent a retting process as preparation of the raw materials. Each fiber bundle sample was carefully separated from the set of bundles. The samples were air-dried with moisture contents ranging from 6% to 8% by weight (%wt).

#### Density measurement of fiber bundles

The apparent densities of fiber bundles were measured by using long (>300mm) fiber bundles. Three samples of each fiber species were weighed and diameters and lengths were measured. The fiber diameters were measured using an optical microscope (Micro Square DS-3USV) at 11–83 randomly selected points at  $\times 300$  magnification. The average diameter was calculated. The fiber lengths were measured using a ruler. The volume of the long fiber bundles was calculated by treating the bundle as a cylinder.

#### Morphological/microstructural observation of fiber bundles

The cross section of each fiber bundle was observed using scanning electron microscope (SEM). The samples were covered with a thin layer of gold using a sputter coater before SEM observation (Jeol JSM 5310). The observation was prepared in the secondary electron mode with a beam current of  $34\mu\text{A}$  and an accelerating voltage of 10kV. Images were obtained at magnifications of  $\times 1000$  and  $\times 3500$ . Typical images (10–15 in number) for each fiber were selected through SEM observation for further morphological analysis, i.e. cell wall thickness, lumen diameter, and shape characteristic.

#### Evaluation of cross-sectional area of fiber bundles

The fiber cross-sectional area is an important parameter to determine the fiber tensile strength. The area ( $S_c$ ) for the fiber tensile strength is in practice calculated from fiber diameter ( $d_c$ ) measurements, recorded by optical microscopy, by the following equation:

$$S_c = \frac{\pi d_c^2}{4} \quad (1)$$

However, the fiber cross-sectional areas calculated by Eq. 1 involved some degree of error when the fiber cross sections were not circular. The error of the cross-sectional area measurement obtained by using the average of fiber diameters at several locations was evaluated to determine the error in the tensile strength; the coefficient factors were calculated for evaluation of the error in the cross-sectional area measurement from SEM images.

In this study, the coefficient factor ( $C$ ) is defined as the ratio of the cross-sectional area ( $S_c$ ) of each fiber based on the average of five diameters ( $d_c$ ) (similar to diameter measurement using optical microscope) set at angle intervals of  $36^\circ$ , to the cross-sectional area ( $S_r$ ) determined from a rep-

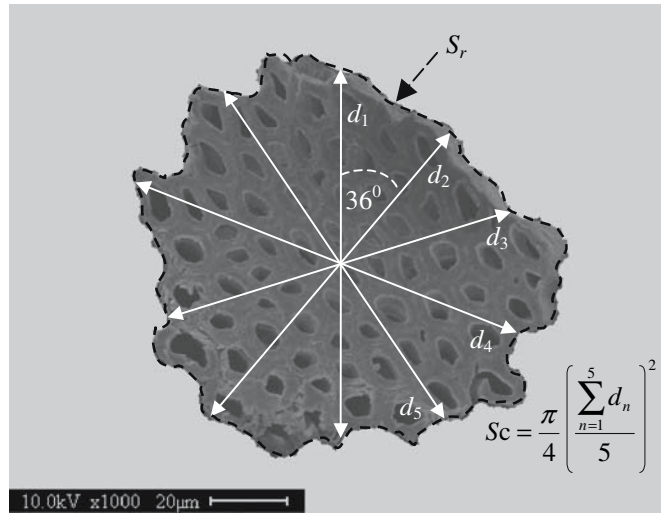


**Fig. 1.** Measurement of cross-sectional area ( $S_c$ ) from the average of five diameter set at angle intervals of  $36^\circ$  and cross-sectional area ( $S_r$ ) as measured by image analysis of scanning electron micrographs

resentative SEM image selected for each fiber by image-analysis software (see Fig. 1) according to the following equation:

$$C = \frac{S_c}{S_r} = \frac{\frac{1}{4}\pi d_c^2}{S_r} \quad (2)$$

#### Preparation of specimens for tensile test

According to the preparation procedure described in ASTM D 3379-75 standard,<sup>4</sup> the fiber bundles were glued to paper frames with 10mm gauge length. The total number of test specimens was in the range of 139–194 for each species, and each was cut into lengths of 20–25 mm. Then the diameters of each specimen at five randomly selected locations were measured using an optical microscope at  $\times 300$  magnification.

Prior to mechanical testing, fiber specimens were again conditioned at 60% relative humidity and at  $20^\circ\text{C}$  for 1 week. The moisture content of each fiber specimen after conditioning varied from 6% to 9%. Following the ASTM D-882 standard, the mechanical properties of fibers were determined using a universal testing machine (Instron 4411) with a crosshead speed of 1mm/min. Before testing, the edge of the supporting paper was cut in the middle. The specimens that fractured at the end of the paper frame or near the glue clamp were excluded from the data for the tensile test.

#### Statistical analysis

Data obtained from the physical and mechanical measurements were statistically assessed using analysis of variance ( $P < 0.05$ ). Error bars in graphs refer to 95% confidence intervals.

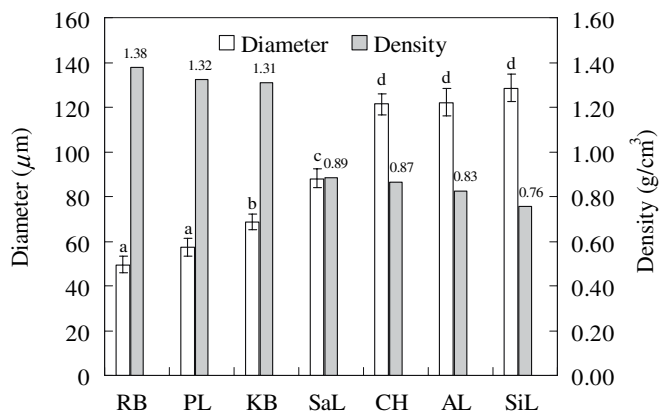


**Fig. 2.** Diameters and densities of seven nonwood plant fiber bundles. Error bars show 95% confidence intervals of mean diameters. Bars marked with different letters are significantly different by Tukey's test ( $P < 0.05$ ). *RB*, ramie bast fiber; *PL*, pineapple leaf fiber; *KB*, kenaf bast fiber; *SaL*, sansevieria leaf fiber; *CH*, coconut husk fiber; *AL*, abaca leaf fiber; *SiL*, sisal leaf fiber

## Results and discussion

### Physical properties

Part of the problem in obtaining a reliable value for density is related to the porous nature of the fibers. Figure 2 shows the diameters and densities of plant fiber bundles. RB had the highest density of  $1.38 \text{ g/cm}^3$  while SiL had the lowest density of  $0.76 \text{ g/cm}^3$ . These values are similar to data published by other authors.<sup>5–10</sup> Baley<sup>11</sup> mentioned that the lumen size for flax fiber bundles increased with increasing diameter. Increasing the lumen size will make the porosity of the fiber increase, and the density of the fiber will decrease. The data on Fig. 2 shows that the density of the fiber decreases with increasing fiber bundle diameter.

Analysis of variance showed that the difference in the average diameter of the fiber species is significant as shown in Table 1. RB provides the lowest and SiL the highest average diameter values. Each fiber species had an average coefficient of variance for the diameter within the specimen of less than 10%, which shows rather uniform diameter.

The diameter distribution of each fiber is shown in Fig. 3. RB, PL, and KB had similar distributions of diameter from 17.2 to  $108.4 \mu\text{m}$ , and SaL had a distribution of diameter from 36.6 to  $138.2 \mu\text{m}$ . AL, CH, and SiL had similar distributions of diameter from 55.6 to  $197.6 \mu\text{m}$ . Figure 3 shows that the diameter of each fiber specimen was normally dispersed, and was able to fulfill the requirement of statistical analysis.

### Morphological/microstructural characteristics

The cross-sectional shape of fiber varied widely from noncircular shapes such as a kidney bean shape for cotton and reasonably circular for wool.<sup>12</sup> Figure 4 shows the differences of cross-sectional image of each fiber. Ordinarily, fibers are bundles, and the fiber bundle size depends mainly

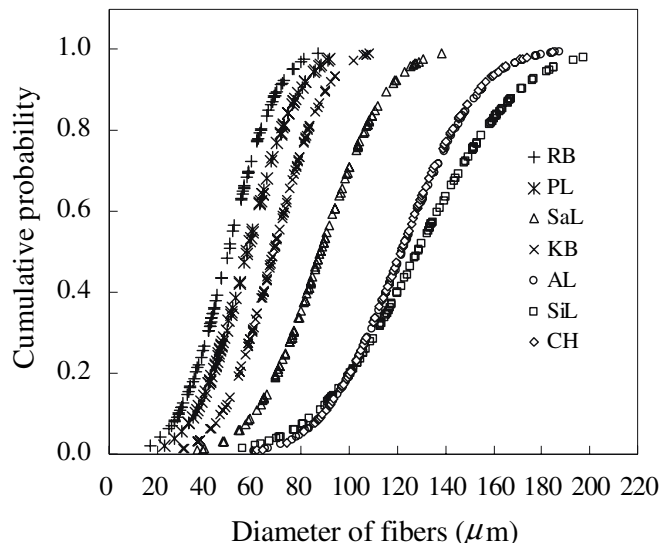


**Fig. 3.** Diameter distributions of the nonwood plant fiber bundles

**Table 1.** Diameters of the nonwood plant fiber bundles

Fibers	$d_o$ among specimens ( $\mu\text{m}$ )	Average CV of diameter within specimens (%)	CV of $d_o$ among specimens (%)
RB	$49.6 \pm 3.6$ a	9.8	32.5
PL	$57.5 \pm 3.9$ a	5.0	29.8
KB	$68.5 \pm 3.4$ b	3.4	24.6
SaL	$88.0 \pm 4.3$ c	6.2	24.9
AL	$122.1 \pm 6.2$ d	4.4	25.7
SiL	$128.6 \pm 6.4$ d	4.2	20.8
CH	$121.3 \pm 4.9$ d	3.9	20.8

Data are given as averages and 95% confidence interval. Values in column with different letters are significantly different by Tukey's test ( $P < 0.05$ )

CV, Coefficient of variation;  $d_o$ , average diameter; RB, ramie bast fiber; PL, pineapple leaf fiber; KB, kenaf bast fiber; SaL, sansevieria leaf fiber; AL, abaca leaf fiber; SiL, sisal leaf fiber; CH, coconut husk fiber

on the number of single fibers in each bundle.<sup>13</sup> The bundle shape, single fiber shape, and lumen diameter of each species are different. All fibers except CH exhibited noncircular shapes on the cross section of fiber bundles. RB showed smaller bundle diameter than the other fibers, while that of SiL was larger.

In generally, cell wall thickness and lumen diameter of fibers varied in the range of  $1\text{--}5 \mu\text{m}$  and  $0.1\text{--}18 \mu\text{m}$ , respectively. All the cross-sectional shapes of single fibers provided were polygonal to round. The differences of single fiber shape and lumen diameter strongly influence fiber density and mechanical and dimensional properties.<sup>14</sup>

### Evaluation of cross-sectional area of fiber bundles

Three techniques are commonly used for fiber diameter characterization, i.e., light microscopy, laser diffraction, and SEM. Laser diffraction and SEM are more accurate than

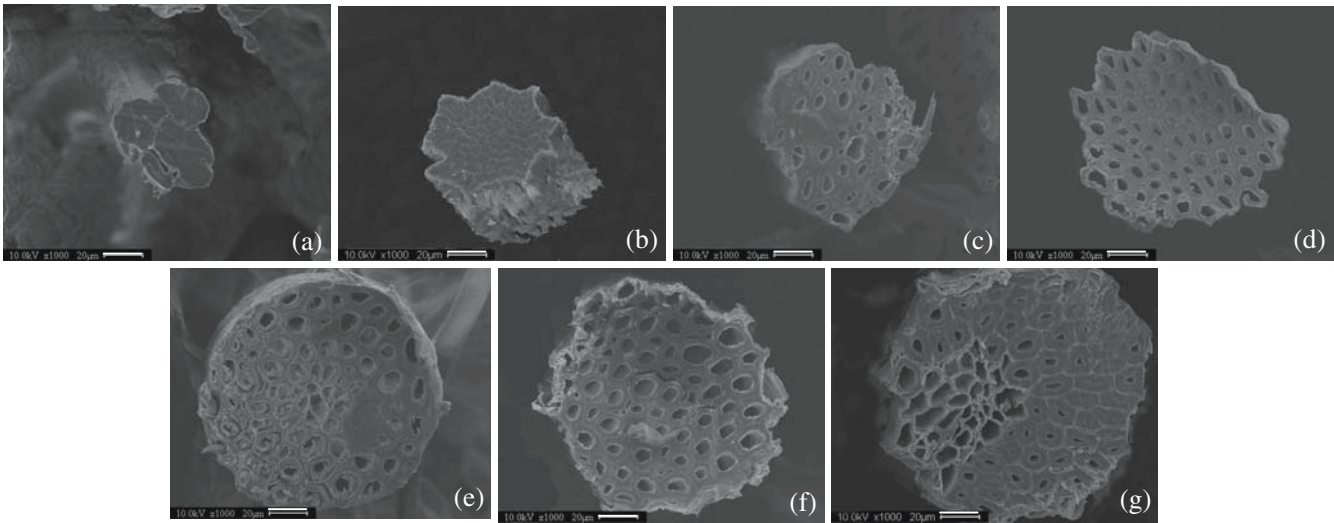


**Fig. 4a–g.** Scanning electron micrographs showing typical shape of cross section in the nonwood plant fiber bundles at  $\times 1000$  magnification. **a** RB, **b** PL, **c** KB, **d** SaL, **e** CH, **f** AL, **g** SiL. Bars  $20\ \mu\text{m}$

light microscopy and can also characterize diameter variations on a smaller scale along the length of the fiber. The difference between diameters measured by laser diffraction and SEM is not statistically significant within the range exhibited by forcibly silked major ampullate fibers from mature *Nephila clavipes* spiders.<sup>15</sup>

Perez et al.<sup>16</sup> characterized *Bombyx mori* cross-sectional geometry by SEM analysis. SEM images were taken from fibers after tensile testing. To allow for variations in the cross-sectional area and shape, the apparent diameter was measured on micrographs recorded at two different positions along the sample ( $0^\circ$ – $50^\circ$ ). The orientation was changed by rotating the sample about its long axis in the microscope, although a rotation of  $90^\circ$  could not be reached because of limited rotation of the microscope. The shape anisotropy of *B. mori* fiber has a range of 1.1–1.5. Selivanova et al.<sup>17</sup> also characterized the coefficient factor of polyacrylonitrile fibers that have a bean-shaped cross-sectional area using an optical microscope and gravimetrically, and obtained a range of 1.26–1.54.

Figure 5 shows the coefficient factor  $C$  of fiber cross-sectional area for the seven samples in the range of 0.92–0.96. The values of  $S_c$  are 4%–8% lower than those of  $S_r$ . Thereby, the coefficient factors of each fiber have little influence in evaluating  $S_o$ . In our research,  $S_o$  has been used directly for the determination of fiber strength.

### Tensile strength

Typical stress–strain curves of the fibers obtained during tensile testing are shown in Fig. 6. The curves show yielding followed by plastic deformation until breakage from 2%–24% strain/elongation for each fiber. The curves of RB, PL, SaL, KB, AL, and SiL have a low strain (2%–6%) and high stress, but the CH curve has a high strain (24%) and low stress. Tensile strength and Young's modulus of RB are higher than other fibers.

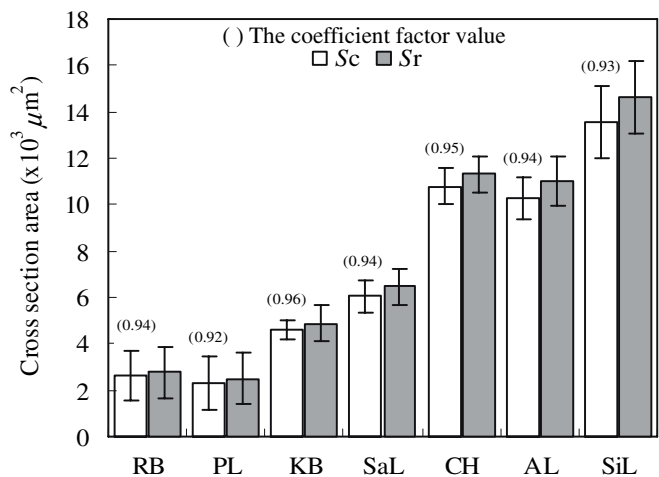


**Fig. 5.** Cross-sectional areas  $S_c$  and  $S_r$  of the nonwood plant fiber bundles and the calculated coefficient factors of cross-sectional area measurement

Up to 0.25% elongation, the testing machine took up lateral slack obtained when the sample was placed in the grip. The fibers exhibited linear stress–strain character up to failure. Every fiber showed a different initial curve shape. The toughness was calculated by integrating the area under the stress–strain curve. High toughness values were obtained for CH (21.5 MPa) and RB (16 MPa) (Table 2).

The mechanical properties of nonwood plant fiber bundles are shown in Table 2 and Fig. 7. RB provides higher values of the average tensile strength and Young's modulus than other fibers, i.e., 849 MPa and 28.4 GPa, respectively. The tensile strength of RB is higher than that of steel (760 MPa), aluminum (200 MPa), polypropylene (80 MPa), nylon (75 MPa), pinewood (40 MPa), and rubber wood (15 MPa), but lower than that of spider silk (1.2 GPa). In addition, the Young's modulus of RB is higher than oak solid wood (11 GPa), polypropylene (2 GPa), polyethylene



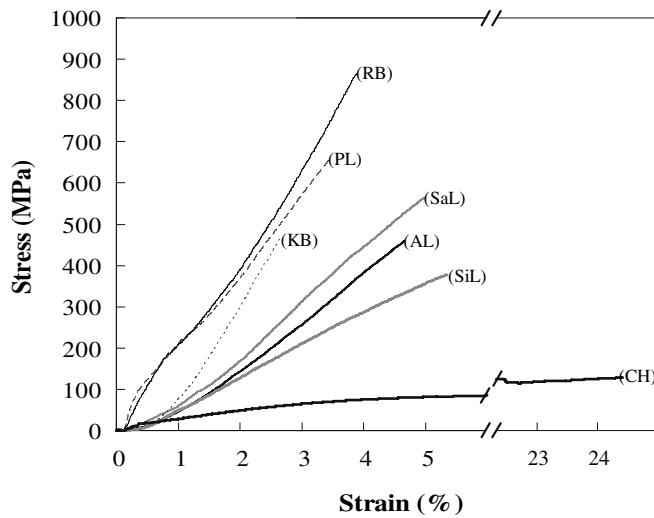


**Fig. 6.** Typical stress-strain curves for the nonwood plant fiber bundles

(2.5 GPa), and polystyrene (3.5 GPa), but lower than that of aluminum (70 GPa).<sup>18</sup> According to Fig. 5,  $S_e$  was 4%–8% lower than  $S_r$ , so the tensile strength and Young's modulus are expected to be decreased by 4%–8% when calculated with  $S_r$ .

High values of specific tensile strength were obtained for SaL (631 MPa) and RB (615 MPa), while high values of specific Young's modulus were obtained for RB (20.6 GPa) and PL (20.5 GPa). Analysis of variance showed that the differences in the tensile strength and Young's modulus of the fibers are significant ( $P < 0.05$ ). The large confidence interval in the mechanical properties of fibers (Table 2) indicated the large variation in the mechanical properties of fibers, which is often observed for natural fibers as found in the data published by other authors.<sup>19–21</sup>

In order to evaluate the large variation in the mechanical properties, plots of mechanical properties versus diameter of the fiber specimens are presented in Fig. 8. The plots

**Fig. 7a, b.** Comparison of **a** the tensile strength and Young's modulus, and **b** the specific tensile strength and specific Young's modulus of the nonwood plant fiber bundles. Error bars show the 95% confidence intervals of the means of tensile strength and Young's modulus

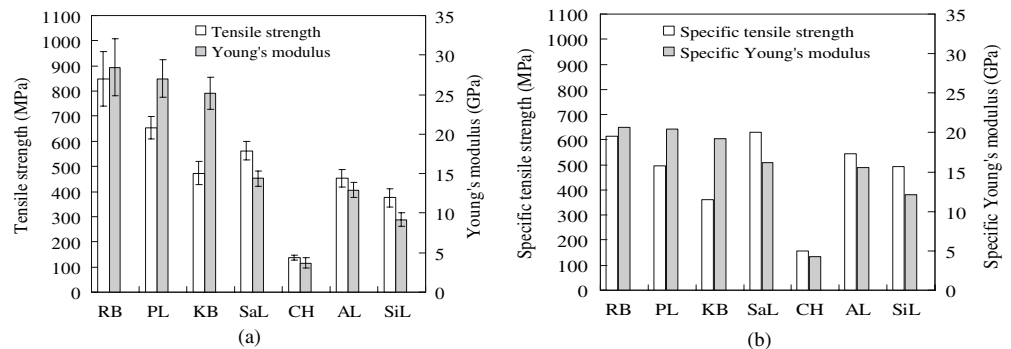


**Fig. 8.** Relationship between diameter and mechanical properties of nonwood plant fiber bundles. **a** Tensile strength, **b** Young's modulus

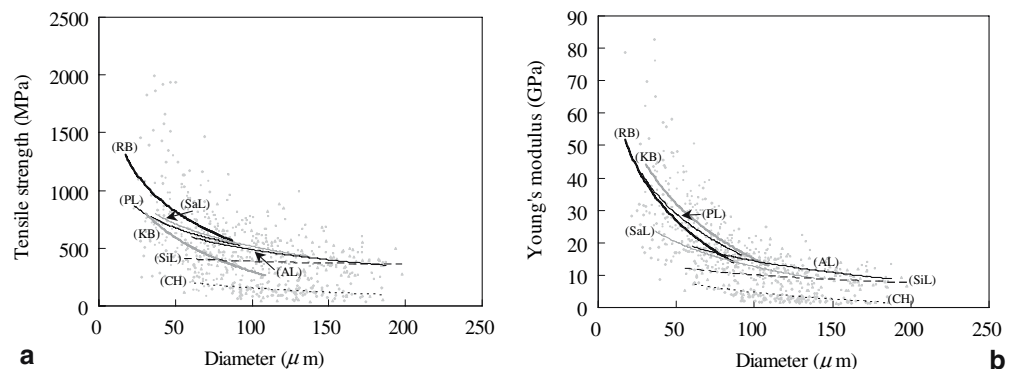


**Table 2.** Mechanical properties of the nonwood plant fiber bundles

Fiber	Tensile strength (MPa)	Specific tensile strength (MPa)	Young's modulus (GPa)	Specific Young's modulus (GPa)	Toughness (MPa)
RB	849 ± 108 e	615	28.4 ± 3.6 d	20.6	16.0 ± 2.4 c
PL	654 ± 46 d	494	27.0 ± 2.3 d	20.5	9.5 ± 0.8 b
KB	473 ± 46 bc	361	25.1 ± 2.0 d	19.2	5.2 ± 0.7 a
SaL	562 ± 36 cd	631	14.4 ± 0.9 c	16.2	12.5 ± 0.9 b
CH	137 ± 11 a	158	3.7 ± 0.6 a	4.2	21.5 ± 2.4 d
AL	452 ± 34 b	545	12.9 ± 0.9 c	15.6	10.0 ± 1.9 b
SiL	375 ± 38 b	493	9.1 ± 0.8 b	12.1	10.7 ± 1.2 b

Data are given as averages and 95% confidence interval. Values in same column with different letters are significantly different by Tukey's test ( $P < 0.05$ )

show a decreasing trend in the tensile strength and Young's modulus with increasing diameter of the fibers. Similar relationships were found in the case of flax fiber and jute fiber.<sup>11,22</sup>

According to literature studies,<sup>23–27</sup> RB provides small spiral angle (7%–12%), high molecular weight (10000), and rich cellulose content (69%–97%). These properties seem to strongly influence the mechanical behavior of RB fiber.

## Conclusions

Morphological characteristics and physical and mechanical properties were determined for seven nonwood plant fiber bundles. The values of the coefficient factor of the cross-sectional area of fiber bundles were in the range of 0.92–0.96. The mechanical properties of fibers showed increasing trends with decreasing diameter. According to the mechanical properties of the fibers, ramie bast, pineapple leaf, and sansevieria leaf showed great potential for use in high-performance plant fiber composites.

**Acknowledgments** The authors thank Prof. Junji Sugiyama, Dr. Misao Yokoyama, Mr. Fumio Kurosaki (RISH, Kyoto University, Japan) for their assistance with SEM; and Mr. Agung B Ismadi (PT Agrina Prima, Jakarta), Mr. Budi Santoso (Center for fiber research, Malang), Mr. Tatang (The Association of natural fibers, Subang) in Indonesia for supplying the seven nonwood plant fiber bundles.

## References

- Kessler RW, Kohler R (1996) New strategies for exploiting flax and hemp. *Chemtec* 26:34–42
- Bledzki AK, Gassan J (1999) Composites reinforced with cellulose based fibres. *Prog Polym Sci* 24:221–274
- Nechtawal A, Mieck K-P, Reussmann T (2003) Developments in the characterization of natural fiber properties and in the use of natural fibers for composites. *Compos Sci Technol* 63:1273–1279
- American Society for Testing and Materials (1978) ASTM D 3379-75 standard test method for tensile strength and Young's modulus for high-modulus single-filament materials. ASTM, Philadelphia, pp 847–852
- Chand N, Hasmi SAR (1993) Effect of plant age on structure and strength of sisal fibre. *Met Mater Process* 5:51–57
- Belmares H, Barrera A, Castillo E, Verheugen E, Monjaras M, Patfoort GA, Bucquoye MEN (1981) New composite materials from natural hard fibers. *Ind Eng Chem Prod Res Dev* 20:555–561
- Paul A, Sabu T (1997) Electrical properties of natural-fiber-reinforced low density polyethylene composites: a comparison with carbon black and glass-fiber-filled low density polyethylene composites. *J Appl Polym Sci* 63:247–266
- Joseph PV, Marcelo SR, LHC Mattoso, Kuruvilla J, Sabu T (2002) Environmental effects on the degradation behaviour of sisal fiber reinforced polypropylene composites. *Compos Sci Technol* 62:1357–1372
- Sanjuan MA, Toledo Filho RD (1998) Effectiveness of crack control at early age on the corrosion of steel bars in low modulus sisal and coconut fibre-reinforced mortars. *Cement Concrete Res* 28:555–565
- Mishra S, Amar KM, Lawrence TD, Manjusri M, George H (2004) A review of pineapple leaf fibers, sisal fibers and their biocomposites. *Macromol Mater Eng* 289:955–974
- Baley C (2002) Analysis of the flax fibers tensile behaviour and analysis of the tensile stiffness increase. *Compos Part A Appl Sci* 33:939–948
- Goswami BC, Rajesh DA, David H (2004) Textile sizing. Marcel Dekker, New York, pp 27–28
- Tao W, Calamari TA, Shih FF, Cao C (1997) Characterization of kenaf fiber bundles and their nonwoven mats. *TAPPI J* 80:162–166
- Yamada J (2002) Radiative properties of fibers with non-circular cross sectional shapes. *J Quant Spectrosc Radiat Transfer* 73:261–272
- Dunaway DL, Thiel BL, Srinivasan SG, Viney C (1995) Characterizing the cross-sectional geometry of thin, non-cylindrical, twisted fibres (spider silk). *J Mater Sci* 30:4161–4170
- Perez-Rigueiro J, Elices M, Llorca J, Viney C (2001) Tensile properties of silkworm silk obtained by forced silking. *J Appl Polym Sci* 82:1926–1935
- Selivanova LF, Polatovskaya RA (1977) Area of an irregular fibre cross section. *Fiber Chem* 9:170–172
- Howatson AM, Lund PG, Todd JD (1992) Engineering tables and data. Kluwer, London, p 41
- Pickering KL, Abdella A, Ji C, McDonald AG, Franich RA (2003) The effect of silane coupling agents on radiata pine fiber for use in thermoplastic matrix composite. *Compos Part A Appl Sci* 34:915–926
- Hornsby PR, Hinrichsen E, Trivedi K (1997) Preparation and properties of polypropylene composites reinforced with wheat and flax straw fibers. Part II. Analysis of composite microstructure and mechanical properties. *J Mater Sci* 32:1009–1015
- Shibata M, Takachiyo K, Ozawa K, Yosomiya R, Takeishi H (2002) Biodegradable polyester composites reinforced with short abaca fiber. *J Appl Polym Sci* 85:129–138
- Zhang M, Kawai S, Sasaki H (1994) Production and properties of composite fiberboard I. Influence of mixing ratio of jute/wood fiber on the properties of boards. *Mokuzai Gakkaishi* 40:816–823
- Bledzki AK, Gassan J (1994) Composites reinforced with cellulose based fibers. *Prog Polym Sci* 24:221–274
- Fengel D, Wegener G (1984) Wood: chemistry, ultrastructure, reactions. Walter de Gruyter, Berlin, p 88
- Angelini LG, Lazzeri A, Levita G, Fontanelli D, Bozzi C (2000) Ramie [*Bohmeria nivea* (L) Gaud] and Spanish broom (*Spartium junceum* L.) fibers for composite materials: agronomical aspects, morphology and mechanical properties. *Ind Crop Prod* 11:145–161
- Yamanaka A, Yoshikawa M, Abe S, Tsutsumi M, Oohazama T, Kitagawa T, Fujishiro H, Ema K, Izumi Y, Nishijima S (2005) Effect of vapor-phase-formaldehyde treatments on thermal conductivity and diffusivity of ramie fibers in the range of low temperature. *J Polym Sci Part B Polym Phys* 43:2754–2766
- Kozloswki R, Rawluk M, Barriga-Bedoya J (2005) Ramie. In: Bast and other plant fibres. Woodhead, Cambridge, UK, p 211